Electronic structure of hcp metals

P. Blaha and K. Schwarz
Institut für Technische Elektrochemie, Technische Universität Wien, A-1060 Vienna, Austria

P. H. Dederichs
Institut für Festkörperforschung, Kernforschungsanlage Jülich, D-5170 Jülich, Federal Republic of Germany
(Received 29 December 1987)

The electronic structure of the hexagonal-closed-packed elements Be, Mg, Sc, Ti, Co, Zn, Y, Zr, Tc, Ru, and Cd is calculated self-consistently by means of the full potential linearized augmented-plane-wave method. Energy-band structures, total and partial densities of states, as well as electron densities are presented and discussed in context with available experimental and theoretical data. Our results confirm that most of the older non-self-consistent calculations obtained realistic energy-band structures, while calculations based on the quantum-defect method generally yield completely different results.

I. INTRODUCTION

The hexagonal-close-packed (hcp) structure is very common among metals, but this structure is more complex than that of the cubic metals. It is for this reason that most of the theoretical investigations are restricted to cubic structures.[1] Furthermore, deviations from the ideal c/a ratio of 1.63 may impose anisotropies, which make the common muffin-time (MT) approximation less reliable. A number of band-structure calculations[2–34] on hcp metals have been published, but most of them are not self-consistent and depend on the starting potential or are performed with various other approximations. For some elements several Fermi surface (FS) models exist or other open problems remain, such as the question whether or not the d band of Cd overlaps the sp bands as it does in Zn. The quantum-defect (QD) method applied by an Indian group[7,12,16] to several elements yields systematically different results than older non-self-consistent $X\alpha$ calculations.

In this paper we shall consider all hcp metals up to Cd. We will restrict ourselves to a scalar relativistic description of the electronic structure and use the self-consistent full potential linearized augmented plane-wave (LAPW) method. Thus we avoid the common MT or atomic sphere approximation (ASA), which may yield less reliable results in this class of metals.[2]

Trends in the electronic structure of the sp metals (Be,Mg,Zn,Cd), the $3d$ series (Sc,Ti,Co) and the $4d$ metals (Y,Zr,Tc,Ru) are described as well as their band structures, densities of states (DOS), and electron densities.

II. METHOD

The present calculations are based on the local-density approximation (LDA) with a parametrization according to Janak.[35] The well-known LAPW method[36] in a scalar relativistic version[37] is employed. The potential and the charge density are allowed to be of arbitrary shape, i.e., no MT approximation is made. Inside the atomic spheres the potential and the charge density is expanded into lattice harmonics (up to $L=6$) and in the interstitial region a Fourier representation is chosen,

$$V(\mathbf{r})=\begin{cases}\sum_{L,M} V_{LM}(r)Y_{LM}(\hat{\mathbf{r}}), & r<R_t\\ \sum_{\mathbf{K}} V_{\mathbf{K}}\exp(i\mathbf{K}\cdot\mathbf{r}), & r>R_t\ .\end{cases}$$

Our method follows the description given earlier[2] except that we now use about 800 $\mathbf{k}$ points in the irreducible wedge of the Brillouin zone. This dense sampling grid for the valence bands was necessary to obtain a reliable value of the electric field gradient (EFG), which is very sensitive to the $\mathbf{k}$ convergence. A coarser $\mathbf{k}$ grid (28 $\mathbf{k}$ points) is used for the semicore states (e.g., $3s$,$3p$ for the $3d$ elements) without loosing precision. The basis set consists of about 140 plane waves and thus the eigenvalues and wave functions are well converged. The non-muffin-tin terms in the potential in general have a relatively small effect on energy bands or density of states (note the respective comments for Co and Cd), but can be essential for the electron-density distribution and the EFG. Since the latter is caused by anisotropies of the p and d valence wave functions, special attention had to be paid to this aspect.

III. ELECTRONIC STRUCTURE OF THE hcp *sp* METALS

The electronic structure of hcp Be has been investigated by the identical method and the results have been presented in great detail in a separate paper;[2] therefore, they are omitted here. Several band-structure calculations of Mg exist in the literature; however, only recently was a pseudopotential (PP) calculation performed self-consistently,[4] but no bands or DOS were presented. In comparison to non-self-consistent calculations[5–7] we find some differences at the points K or M (see Fig. 1), and in particular in the latter work the second L_1 point is higher than ours. The DOS is in good agreement with the augmented plane-wave (APW) calculation[5] and the PP calcu-

 ©1988 The American Physical Society

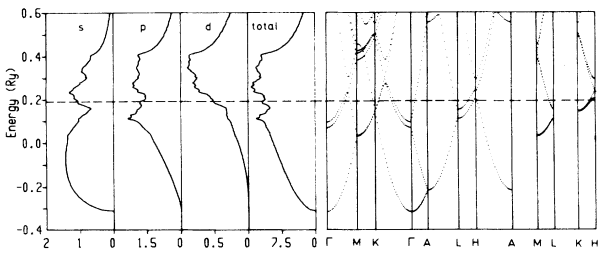

FIG. 1. Density of states and energy bands of hcp Mg. In the panels from left to right the partial s, p, and d DOS [in (states/Ry)/atom] and the total DOS [in (states/Ry)/unit cell] are given.

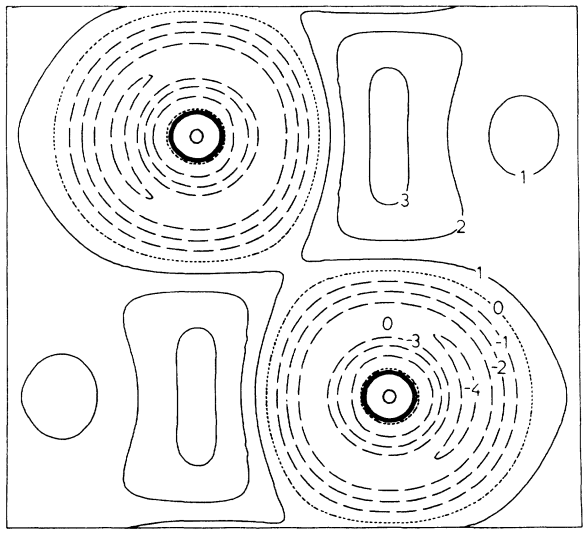

FIG. 2. Difference electron densities of hcp Mg in the $(11\bar{2}0)$ plane. Units of $0.001e$/a.u.^{3} are used.

lation by Rennert *et al.*,[8] while the quantum-defect method by Chatterjee and Singha[7] and Korringa-Kohn-Rostoker (KKR) calculation[6] obtain the Fermi energy at the major peak in their DOS. Our ratio of the $(p_x,p_y)/p_z$ charge is 2.03 (Table I) and thus very close to a completely spherical charge-density distribution. This was also found in the recent PP calculation by Chou and Cohen,[4] although they report slightly different values for p_x and p_y, which should be degenerate for hcp symmetry. A difference electron density as the one shown in Fig. 2, which is defined as the difference between the crystalline electron density and a density obtained by superposition of spherical neutral atoms, can display fine details, such as small anisotropies, expansions, or contractions of wave functions relative to an atomic reference state, effects not detectable in the total density. The difference electron density of Mg shows almost no deviation from spherical symmetry, but a more diffuse crystalline charge density than that from superposed atoms. This is due to a partial promotion of the $3s$ electrons into $3p$ states. It is this nearly spherical charge distribution which leads to the small EFG value observed in Mg as reported in Ref. 3.

Hcp Zn and Cd are special, since they are the only elements which crystallize with an extremely large c/a ratio (1.86 and 1.89, respectively). The FS is well explained by empirical PP calculations[9] or non-self-consistent $X\alpha$ calculations,[10,11] but as well by our band structure (Fig. 3) which agrees well with these previous ones. The d states completely overlap with the valence sp bands and therefore should not be treated as core states. The QD method applied by Sinha and Chatterjee[12] yields bands such that at L the third and fourth bands are occupied and a peak in their DOS is present at the Fermi energy in contrast to our calculation, where the Fermi energy falls near a local minimum of the sp band DOS. The difference electron density shown in Fig. 4 presents a positive density in the interstitial region as in Mg, but the negative density near the nucleus is no longer spherically symmetric but shows large anisotropies as can be seen clearly in the magnification at the right side of Fig. 4. This anisotropy, also apparent in the $(p_x,p_y)/p_z$ ratio of 2.84 (Table I), together with the nodal structure of the $4p$ wave function is responsible for the high EFG in Zn.[3] Since the d states lie well below the Fermi energy, they are fully occupied and their anisotropy is small.

Our band structure of Cd shown in Fig. 5 appears to be the first calculation including d states. In contrast to the MT calculation of fcc Cd,[1] where the d band is separated from the sp valence bands by 0.03 Ry, we find a partial

TABLE I. Partial charges inside the atomic sphere of radius R_{MT} and densities of states at the Fermi level in $n(E_F)$ [in (states/Ry)/cell]. d_{xy} denotes the sum of the degenerate states of d_{xy} and $d_{x^2-y^2}$ symmetry; d_{xz} denotes states of d_{xz} and d_{yz} symmetry.

Element	R_{MT}	s	p	p_z	p_x,p_y	d	d_{z^2}	d_{xy}	d_{xz}	$n(E_F)$
Mg	2.80	0.596	0.491	0.162	0.329	0.068				11.8
Zn	2.25	0.566	0.399	0.106	0.293	9.676	1.939	3.865	3.872	5.4
Cd	2.70	0.705	0.467	0.120	0.347	9.688	1.941	3.873	3.874	6.1
Sc	2.95	0.454	0.348	0.107	0.242	1.222	0.266	0.480	0.476	59.0
Ti	2.60	0.389	0.336	0.105	0.231	2.107	0.472	0.917	0.718	23.8
$Co_\uparrow$	2.00	0.129	0.104	0.035	0.069	4.227	0.838	1.686	1.703	4.4
$Co_\downarrow$	2.00	0.134	0.123	0.042	0.081	2.559	0.513	1.028	1.018	20.8
Y	3.00	0.354	0.207	0.061	0.146	0.967	0.216	0.377	0.374	54.7
Zr	2.75	0.342	0.254	0.077	0.177	1.821	0.409	0.781	0.631	26.0
Tc	2.50	0.392	0.396	0.136	0.260	4.814	0.967	1.932	1.915	24.6
Ru	2.40	0.359	0.371	0.128	0.243	5.717	1.116	2.292	2.309	22.0

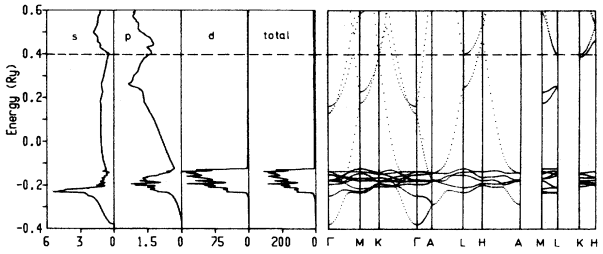

FIG. 3. Density of states and energy bands of hcp Zn (details as in Fig. 1).

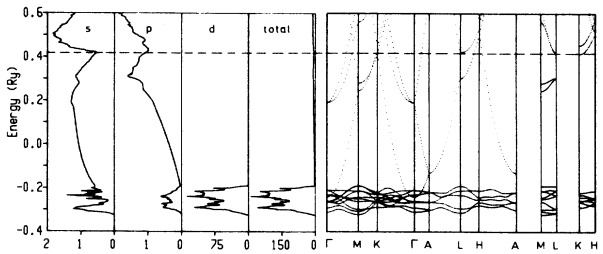

FIG. 5. Density of states and energy bands of hcp Cd (details as in Fig. 1).

overlap. Thus the situation is similar to hcp Zn, but the overlap is smaller in Cd than in Zn. The difference to the fcc MT calculation[1] is primarily due to non-muffin-tin effects, as some test calculations have indicated. The warped interstitial potential lowers the energy of the more diffuse s states relative to the d band. The FS is in good agreement with an empirical PP calculation,[9] while Sinha and Chatterjee[12] find the third and fourth band at L occupied (as in their Zn calculation) and a clear double intersection along the Γ-Σ-M direction due to a noncrossing band, whose interaction appears to be too weak. The latter authors position their d bands below the sp band minimum (both in Zn and Cd) and find the Fermi energy again at a peak in their DOS, while our E_F falls in a minimum of the s-like DOS. The $(p_x,p_y)/p_z$ ratio of 2.95 (Table I) shows an even more pronounced p_x,p_y excess than in Zn, consistent with the somewhat higher c/a ratio and the higher EFG value[6] in Cd compared to Zn. The difference density is very similar to that of Zn shown in Fig. 4 and indicates again how well the density can be described by superposed atoms. Only in the region near the nuclei pronounced differences can be seen, which cannot be detected by x-ray diffraction measurements, but are indirectly observed in the high experimental EFG value.

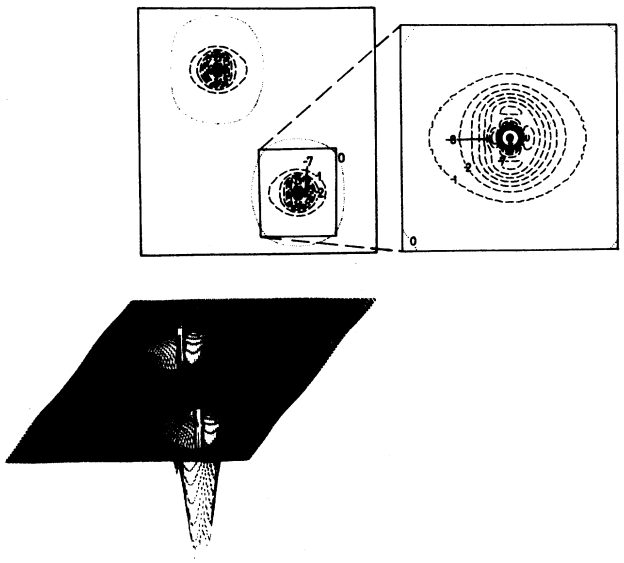

FIG. 4. Difference electron densities of hcp Zn in the $(11\bar{2}0)$ plane. The cutoff of the perspective plot is $0.08e$/a.u.^{3} In the contour plot units of $0.001e$/a.u.^{3} are used.

IV. ELECTRONIC STRUCTURE OF THE hcp 3d METALS

The energy bands of Sc are displayed in Fig. 6 and agree in general with the non-self-consistent earlier APW calculations.[13,14] We find the second L_1 point unoccupied, in agreement with the earlier APW calculation[14] and the FS displayed in Ref. 15. Our results therefore contradict speculations of Schirber *et al.*,[38] that the band positions at Γ and H in non-self-consistent calculations could be shifted when going towards self-consistency. Therefore this effect cannot explain why some of the theoretically predicted frequencies are missing in their de Haas–van Alphen measurements. The most recent APW calculation[13] uses the atomic starting configuration, the exchange-correlation potential, and the calculational method as in Refs. 14 and 15, but finds the second L_1 point occupied. Our DOS agrees well with the earlier calculations. We find the two peaks in the unoccupied DOS at about 1.6 and 3.8 eV above the Fermi energy, which is very close to the experimental findings[39] and agrees much better than the ASW results obtained in the same reference.[39] This disagreement between LAPW and ASW was also found for Y, but not for Ti and Zr, indicating some problems in using the ASW method with the atomic sphere approximation for these first row transition metals. Here as in all other cases, where we have made comparisons, we find various discrepancies between our results and a QD calculation,[16] which for instance yields a third occupied band at Γ and a DOS significantly different to ours. The $(p_x,p_y)/p_z$ ratio of 2.26 (Table I) is much smaller than in Zn or Cd, but still larger than 2, although the c/a ratio is now less than the ideal one, while

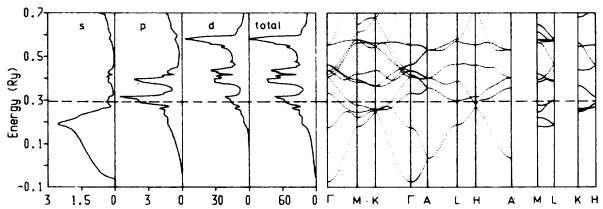

FIG. 6. Density of states and energy bands of hcp Sc (details as in Fig. 1).

it was larger for Zn and Cd. The d electrons are split by symmetry into three groups: d_{z^2}; $d_{xy}, d_{x^2-y^2}$; and d_{xz}, d_{yx} orbitals. The partial d DOS (Fig. 7) shows a slightly larger occupation of d_{z^2} electrons. This is consistent with the integrated partial charges (Table I), which include the degeneracies of the d states and make the d_{z^2} value larger than half the other d-partial charges. In this context we define the deviation from spherical symmetry of the p and d states as polarization Δn_p and Δn_d, namely,

$$\Delta n_p = \tfrac{1}{2}(n_{p_x} + n_{p_y}) - n_{p_z}$$

and

$$\Delta n_d = (n_{d_{xy}} + n_{d_{x^2-y^2}}) - \tfrac{1}{2}(n_{d_{xz}} + n_{d_{yz}}) - n_{d_{z^2}}$$

and find that the d polarization Δn_d is opposite to Δn_p (p_x, p_y excess). The difference density looks very similar to that of Ti (Fig. 9), except that the anisotropies are much smaller (the minima are only about 0.01 electrons/a.u.^{3} deep).

Our energy bands for Ti (Fig. 8) agree well with the relativistic but non-self-consistent linear muffin-tin orbital (LMTO) calculation[17] of Jepsen and the new LAPW calculation by Lu *et al.*[40] We too find the double intersection of the $\Gamma-\Delta-A$ band with the Fermi energy, although these levels are so close to E_F that we cannot make a definite statement. Previous calculations by High and Welch[18] using different starting potentials do not agree, however. A more recent APW calculation[19] yields an occupied valence-band width of only 0.3 Ry compared to 0.45 Ry in our calculation. The $(p_x, p_y)/p_z$ ratio is still higher than 2 (2.19) giving rise to a positive Δn_p. We find about 0.2 d_{xz}, d_{yz} electrons less than for the other symmetries (compare the Sc DOS in Fig. 7 and Table I) and therefore obtain also a positive Δn_d. This anisotropy of the d states is also present in the valence electron densities (peaks in the xy plane and in z direction, minima in xz, yz planes) and in the difference electron densities (Fig. 9), where negative contours with d_{xz}, d_{yz} symmetry dominate. Since the overlap between d functions on nearest-neighbor Ti atoms is small and, furthermore, orbitals with symmetries pointing in these directions are depopulated in comparison to other symmetries, the d—d bond seems not to be very favorable. Again a positive interstitial background in the difference density is present as in the sp metals. Since the valence charge density is highly nonspherical, Ti would be a good system for precise x-ray form factor measurements, where large deviations from the spherical atomic form factors should be found. Note that although the d polarization is an order of magnitude larger than the p polarization, the p contribution to the EFG is more important than the d (48 versus 33×10^{13} esu/cm). This is due to the different radial behavior of $3d$ and $4p$ wave functions near the origin as explained before.[3] Ti and Zr are the only elements investigated here, where the p and d polarization have the same sign.

The electronic structure of hcp Co is studied even less than that of other hcp metals because of the additional ferromagnetism. Attempts were made using paramagnet-

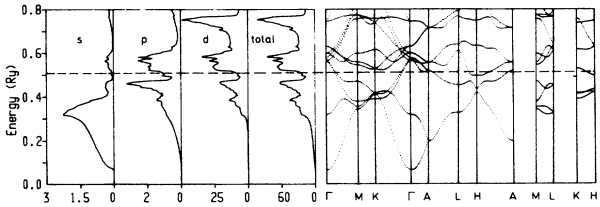

FIG. 8. Density of states and energy bands of hcp Ti (details as in Fig. 1).

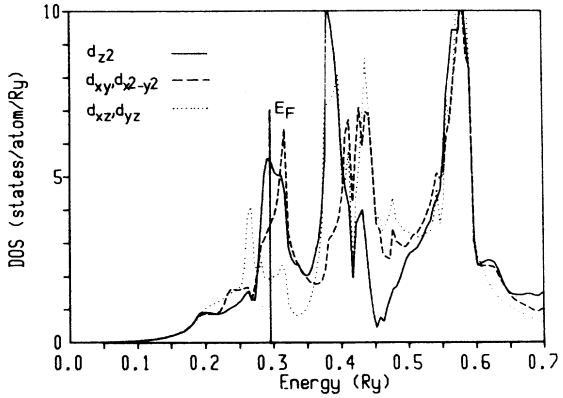

FIG. 7. Symmetry decomposition of the partial d density of states of hcp Sc [in (states/atom)/Ry] normalized to one d state (without degeneracy).

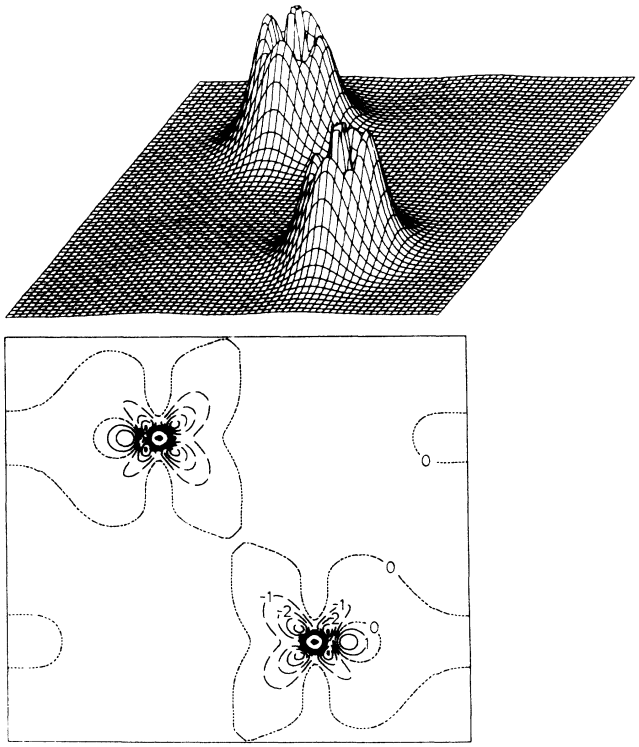

FIG. 9. Top: Perspective plot of the valence electron densities of hcp Ti in the $(11\bar{2}0)$ plane. Cutoff at $0.25e$/a.u.^{3}. Bottom: Contour plot of the difference electron densities of hcp Ti in the $(11\bar{2}0)$ plane. Units of $0.01e$/a.u.^{3} are used.

ic calculations and a rigid shift approximation for spin-up and -down bands (Batallan *et al.*[20]) or using adjusted exchange-correlation potentials (Kulikov and Kulatov[21]). A Hartree-Fock (HF) calculation, including correlation effects[22] was also performed. The only self-consistent local-spin-density-functional (LSDF) calculation, which gives a detailed discussion of the electronic structure of hcp Co, is the recent LMTO calculation by Jarlborg and Peter.[23] The exchange splitting found experimentally[41] is about 1 eV and was used together with the magnetic moment ($1.58\mu_B$) as input for the earlier investigations. We find an exchange splitting of about 1.55 eV and a moment of $1.595\mu_B$, while two other LMTO calculations[23,25] yield 1.55 and 1.63 μ_B, respectively, and a recent relativistic calculation[24] found $1.50\mu_B$ for the spin and $0.15\mu_B$ for the orbital moment. The exchange splitting of about 4 eV in the HF calculation is much too high. The spin-up bands (Fig. 10) agree reasonably well with all previous calculations and with photoemission experiments,[41] except at the Γ_{3+} point, which in experiment is placed 1.15 eV below E_F but only 0.1 eV according to our calculation. Our spin-up FS is in qualitative agreement with previous work without a necessity to reduce the exchange splitting to the experimental value of 1 eV. Jarlborg and Peter[23] find no neck in the FS at Γ, because they place Γ_{3+} 0.16 eV above E_F. This difference could be caused by the ASA used in their calculation. The situation with the spin-down bands (Fig. 11) is even more complicated, since E_F falls right into the d-band complex. The Γ_{3+} state is unoccupied in the present and in all previous calculations except the calculation by Kulikov and Kulatov,[21] giving rise to a small hole ball in the FS around Γ. On the other hand, photoemission data[41] are interpreted assuming non-spin-splitted Γ_{3+} states placed 1.15 eV below E_F, but even Kulikov and Kulatov find their Γ_{3+} state much closer to E_F and already unoccupied at a pressure of 290 kbar. The situation around L is even more complex. We find L_2 below E_F giving rise to a fairly simple FS around L, which is in agreement with the other LSDF calculation.[23] In addition, we find a small pocket around the U symmetry line (close to L), as was found earlier by Wakoh and Yamashita[26] and suggested experimentally (although with some doubts).[42] All other calculations find L_2 unoccupied and a fairly complicated FS, but it should be noted that even semiempirical calculations yield FS which do not agree well with experiment, as the large discrepancies at the γ or ϵ orbits in Ref. 21 indicate. It should be noted that the energy differences are very small and better density functionals and/or the

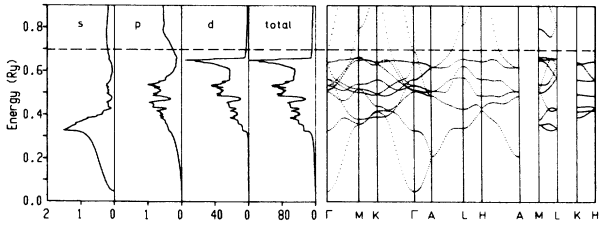

FIG. 10. Spin-up density of states and energy bands of hcp Co (details as in Fig. 1).

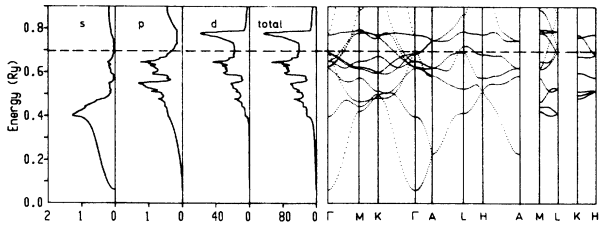

FIG. 11. Spin-down density of states and energy bands of hcp Co (details as in Fig. 1).

spin-orbit coupling could change the FS qualitatively as well as quantitatively. The total DOS (Figs. 10 and 11) and the DOS at the Fermi energy, $n(E_F)$ (Table I) agree well with previous calculations. Experimental bremsstrahlung isochromat spectroscopy (BIS) spectra[39] find a peak at 0.5 eV above E_F. We find this peak 0.9 to 1.0 eV above E_F, which is consistent with the theoretical overestimation of the spin splitting by about 0.5 eV. We do not understand the theoretical results in Ref. 39, which find the peak position in perfect agreement with experiment in contradiction to all other LDA calculations. The $(p_x,p_y)/p_z$ ratio (Table I) for spin-up and spin-down is 1.97 and 1.93, respectively, and close to spherical symmetry. The $d_{xz,yz}$ spin-up electrons show a slight excess ($0.02e^-$), but the spin-down electrons compensate it, so that all d states are almost spherically symmetric. The spin density (Fig. 12) shows the spatially localized moment arising from the d states with the very small anisotropy caused by the different occupations mentioned

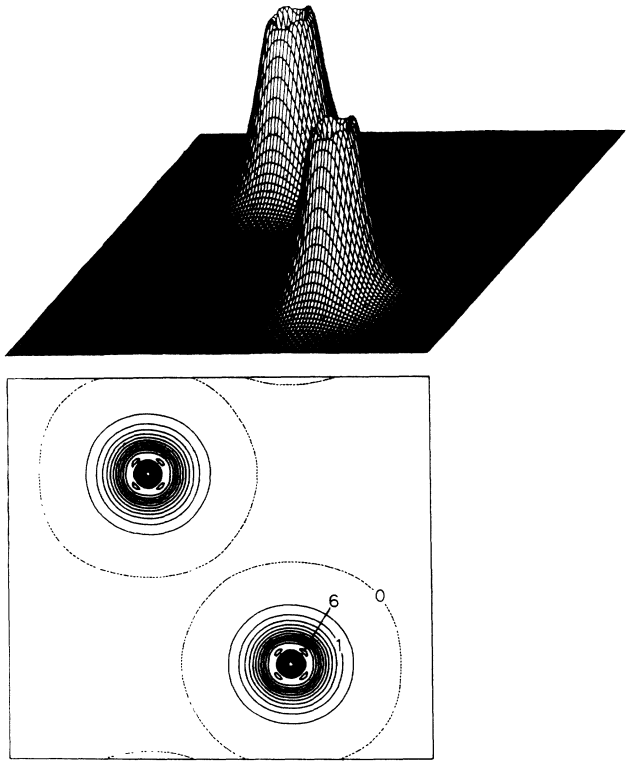

FIG. 12. Spin densities of hcp Co in the $(11\bar{2}0)$ plane. Units of $0.1e$/a.u.^{3} are used in the contour plot.

above and the negative s and p polarization (as in Fe and Ni) in the interstitial region. This compares favorably with polarized neutron scattering data on Co.[43] Our hyperfine field, calculated from nonrelativistic wave functions,[44] is -229 kG and is therefore in good agreement with the experimental value of -223 kG. The HF calculation[22] finds a very large value of -423 kG and the LMTO calculation[23] yields 291 kG. A decomposition of this hyperfine field into contributions from different states exhibits the importance of the core electrons and shows the partial cancellation of the positive $3s$ and the negative $1s,2s$ contributions ($1s,2s$: -396 kG; $3s$: $+231$ kG; valence: -64 kG).

V. ELECTRONIC STRUCTURE OF THE hcp 4d METALS

The electronic structure of hcp Y has been calculated previously by Loucks[27] by means of the non-self-consistent APW method, but he did not publish the energy-band structure. Our energy bands and the total as well as the partial DOS are shown in Fig. 13. It turns out that our FS is in good agreement both with experiment[45] and Loucks's FS model.[27] In addition we find a larger α orbit of 5.7×10^7 G in agreement with experiment. The metals Y and Sc exhibit the highest $n(E_F)$ of all hcp metals investigated (Table I). Similar to Sc we find peak positions in the unoccupied DOS at 1.6 and 5.1 eV above the Fermi energy in much better agreement with the experimental results[39] than with their theoretical results. The p anisotropy ratio is 2.39 and thus a relatively high EFG of $+93\times10^{13}$ esu/cm^3 is predicted. No experimental value of this EFG is available, but an empirical model calculation[46] predicted a negative value, which—contrary to our results—would be opposite in sign to the values for Sc, Ti, and Zr.

The energy bands of Zr have been studied by various authors. Our results (Fig. 14) are in very good agreement with the results of Jepsen *et al.*[28] and Lu *et al.*[40] Thus we also find unoccupied third and fourth bands at A, but occupied fifth and sixth bands at H. Therefore the orbits of the third and fourth zone are open along $\Gamma-A$ in contradiction to experimental interpretations.[47] It should be noted again that energy changes of a few mRy could bring our FS in qualitative agreement with experiment. The $X\alpha$ APW band structure of Chatterjee[29] finds this A point clearly occupied, but his Γ_{3+} point is too close to E_F so that he cannot explain the α or β orbits. In addition, he finds additional intersections along $\Gamma-T-K$ and $L-R-A$, leading to cross sections, which are experimentally not supported. Our DOS (Fig. 14) is in good agreement with Jepsen *et al.*,[28] while another calculation by Vohra *et al.*[19] yields a total valence-band width of only 0.31 Ry. The p anisotropy ratio is 2.29 (similar to Y), but the d electrons are now polarized in the same direction as the p, so that the combined effect adds to a large EFG of 143×10^{13} esu/cm^3.

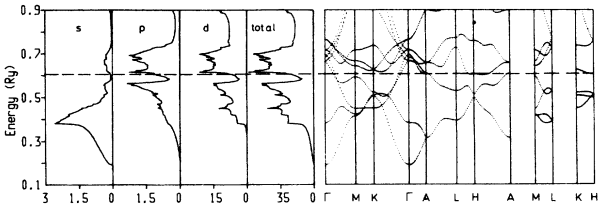

FIG. 14. Density of states and energy bands of hcp Zr (details as in Fig. 1).

Our energy bands of Tc (Fig. 15) are in fair agreement with the KKR calculation by Faulkner.[30] In addition to Faulkner's FS two holes appear at L, since our fifth and sixth bands are unoccupied at L. This was also found in de Haas–van Alphen measurements by Arko *et al.*[48] The energy bands of Chatterjee[31] show several intersections along $M-K$ and a Γ_{3+} state, which is not pushed high enough above E_F compared to our calculation. For these reasons his DOS deviates somewhat from ours and $n(E_F)$ is lower in the present calculation, but in good agreement with Ref. 30. The results by Asokamani *et al.*[32,33] deviate strongly from ours for all the different potential approximations he assumed. The p anisotropy is 1.91 and thus shows a clear p_z excess while the d anisotropy is again opposite to the p (only Ti and Zr show equal p and d polarizations).

The electronic and structural properties of Ru have been investigated recently by a pseudopotential method,[34] and their bands are in fair agreement with previous relativistic bands[28] and ours (Fig. 16). Differences can be seen especially along $\Gamma-T-K$, where in the nonrelativistic calculation some band crossings are avoided similar to the relativistic bands.[28] In terms of the bandwidth or the position of special $\mathbf{k}$ points our scalar relativistic calculation agree better with the fully relativistic non-self-consistent calculation[28] than with the self-consistent nonrelativistic pseudopotential calculation.[34] There is good overall agreement with photoelectron spectroscopy[49] except for a flat band 0.3 eV below E_F in experiment but unexplained in all theoretical papers. The FS is in good agreement with experiment.[50]

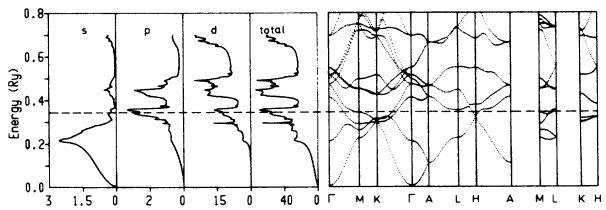

FIG. 13. Density of states and energy bands of hcp Y (details as in Fig. 1).

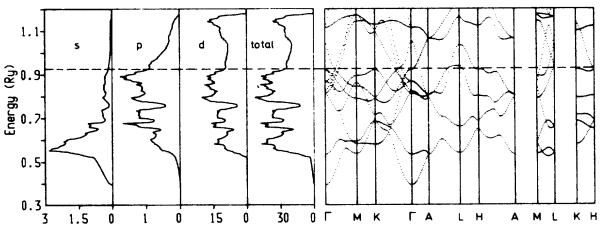

FIG. 15. Density of states and energy bands of hcp Tc (details as in Fig. 1).

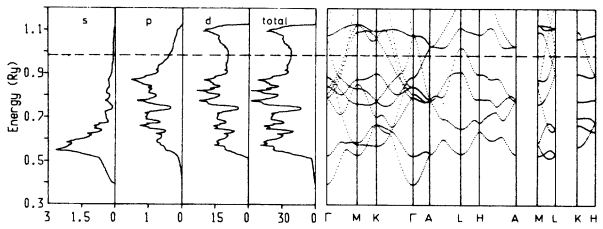

FIG. 16. Density of states and energy bands of hcp Ru (details as in Fig. 1).

VI. SUMMARY

We have calculated the electronic structure of all hcp elements up to Cd by means of the self-consistent full potential LAPW method and thus avoided the common muffin-tin approximation for these anisotropic metals. The energy bands and the total DOS are whenever available compared with previous, mostly non-self-consistent calculations. In many, but not in all cases good overall agreement between the previous $X\alpha$ calculations and the present results is found. Calculations based on the quantum-defect method do not agree at all. In the energy-band structure of hcp Cd we find an overlap between the s and d bands as in Zn. This is in contrast to MT calculations for the fcc structure, where the d band lies below the bottom of the s band in Cd, but overlaps in Zn. Partial DOS and partial charges as well as electron densities are shown and used to interpret chemical bonding. We suggest measurements of x-ray form factors on hcp Ti because of its highly anisotropic d charge density, which should be detectable in such experiments. For hcp Co we obtain a magnetic moment of $1.6\mu_B$ and an exchange splitting of 1.55 eV; the latter being too high with respect to experiment. The spin density is almost spherically symmetric and thus in excellent agreement with experimental data.

ACKNOWLEDGMENT

One of us (P.B.) would like to thank the Kernforschungsanlage Jülich for its support during his stay at Jülich.

[1]V. L. Moruzzi, J. F. Janak, and A. R. Williams, *Calculated Electronic Properties of Metals* (Pergamon, New York, 1978).
[2]P. Blaha and K. Schwarz, J. Phys. F **17**, 899 (1987).
[3]P. Blaha, K. Schwarz, and P. H. Dederichs, Phys. Rev. B (to be published).
[4]M. Y. Chou and M. L. Cohen, Solid State Commun. **57**, 785 (1986).
[5]S. T. Inoue and J. Yamashita, J. Phys. Soc. Jpn. **35**, 677 (1973).
[6]R. Asokamani, K. Iyakutti, R. S. Rao, and V. Devanathan, J. Phys. F **8**, 2323 (1978).
[7]S. Chatterjee and P. Sinha, J. Phys. F **5**, 2089 (1975).
[8]P. Rennert, H. Schelle, and U. H. Glaser, Phys. Status Solidi B **121**, 673 (1984).
[9]R. W. Stark and L. M. Falicov, Phys. Rev. Lett. **19**, 795 (1967).
[10]G. E. Juras, B. Segall, and C. B. Sommers, Solid State Commun. **10**, 427 (1972).
[11]S. Daniuk, Acta Phys. Polonica A **63**, 633 (1983).
[12]P. Sinha and S. Chatterjee, J. Phys. F **7**, 105 (1977).
[13]S. G. Das, Phys. Rev. B **13**, 3978 (1976).
[14]G. S. Fleming and T. L. Loucks, Phys. Rev. **173**, 685 (1986).
[15]J. Rath and A. J. Freeman, Phys. Rev. B **11**, 2109 (1975).
[16]M. Sen and S. Chatterjee, J. Phys. F **10**, 985 (1980).
[17]O. Jepsen, Phys. Rev. B **12**, 2988 (1975).
[18]R. M. Welch and E. H. Hygh, Phys. Rev. B **9**, 1993 (1974) and references therein.
[19]Y. K. Vohra, S. K. Sikka, and R. Chidambaram, J. Phys. F **9**, 1771 (1979).
[20]F. Batallan, I. Rosenman, and C. B. Sommers, Phys. Rev. B **11**, 545 (1975).
[21]N. I. Kulikov and E. T. Kulatov, J. Phys. F **12**, 2267 (1982).
[22]C. M. Singal and T. P. Das, Phys. Rev. B **16**, 5068 (1977).
[23]T. Jarlborg and M. Peter, J. Magn. Magn. Mater. **42**, 89 (1984).
[24]B. I. Min, T. Oguchi, and J. A. Freeman, Phys. Rev. B **33**, 7852 (1986).
[25]B. Szpunar and P. Strange, J. Phys. F **15**, L165 (1985).
[26]S. Wakoh and J. Yamashita, J. Phys. Soc. Jpn. **28**, 1151 (1970).
[27]T. L. Loucks, Phys. Rev. **144**, 504 (1966).
[28]O. Jepsen, O. K. Andersen, and A. R. Mackintosh, Phys. Rev. B **12**, 3084 (1975).
[29]P. Chatterjee, J. Phys. F **14**, 2027 (1984).
[30]J. S. Faulkner, Phys. Rev. B **16**, 736 (1977).
[31]P. Chatterjee, Phys. Rev. B **27**, 4722 (1983).
[32]R. Asokamani, K. Iyakutti, and V. Devanathan, Solid State Commun. **30**, 385 (1979).
[33]R. Asokamani and K. Iyakutti, J. Phys. F **10**, 1157 (1980).
[34]J. R. Chelikowsky, C. T. Chan, and S. G. Louie, Phys. Rev. B **34**, 6656 (1986).
[35]J. F. Janak, Solid State Commun. **25**, 53 (1978).
[36]D. D. Koelling and G. O. Arbman, J. Phys. C **5**, 2041 (1975).
[37]D. D. Koelling and B. N. Harmon, J. Phys. C **10**, 3107 (1977).
[38]J. E. Schirber, A. C. Switendick, and P. A. Schmidt, Phys. Rev. B **27**, 6475 (1983).
[39]W. Speier, J. C. Fuggle, R. Zeller, B. Ackermann, K. Szot, F. U. Hillebrecht, and M. Campagna, Phys. Rev. B **30**, 6921 (1984).
[40]Z. W. Lu, D. Singh, and H. Krakauer, Phys. Rev. B **36**, 7335 (1987).
[41]F. J. Himpsel and D. E. Eastman, Phys. Rev. B **21**, 3207 (1980).
[42]I. Rosenman and F. Batalan, Phys. Rev. B **5**, 1340 (1972).
[43]R. M. Moon, Phys. Rev. **136A**, 195 (1964).
[44]S. Blügel, H. Akai, R. Zeller, and P. H. Dederichs, Phys. Rev. B **35**, 3271 (1987).
[45]P. G. Mattocks and R. C. Young, J. Phys. F **8**, 1417 (1978).
[46]S. Chandra and H. C. Verma, Phys. Status Solidi B **131**, K73 (1985).
[47]P. M. Everett, Phys. Rev. B **20**, 1419 (1979).
[48]A. J. Arko, G. W. Crabtree, S. P. Hörnfeldt, J. B. Ketterson, G. Kostorz, and L. R. Windmiller, in *Proceedings of the Thirteenth International Low Temperature Physics Conference—LT13*, edited by K. D. Timmerhaus, W. J. O'Sullivan, and E. F. Hammel (Plenum, New York, 1974), Vol. 4, p. 104.
[49]F. J. Himpsel, K. Christmann, P. Heimann, and D. E. Eastman, Phys. Rev. B **23**, 2548 (1981).
[50]E. S. Alekseev, V. A. Venttsel, O. A. Voronov, A. I. Likhter, and M. V. Magnitskaya, Zh. Eksp. Teor. Fiz. **76**, 215 (1979) [Sov. Phys.—JETP **49**, 110 (1979)].

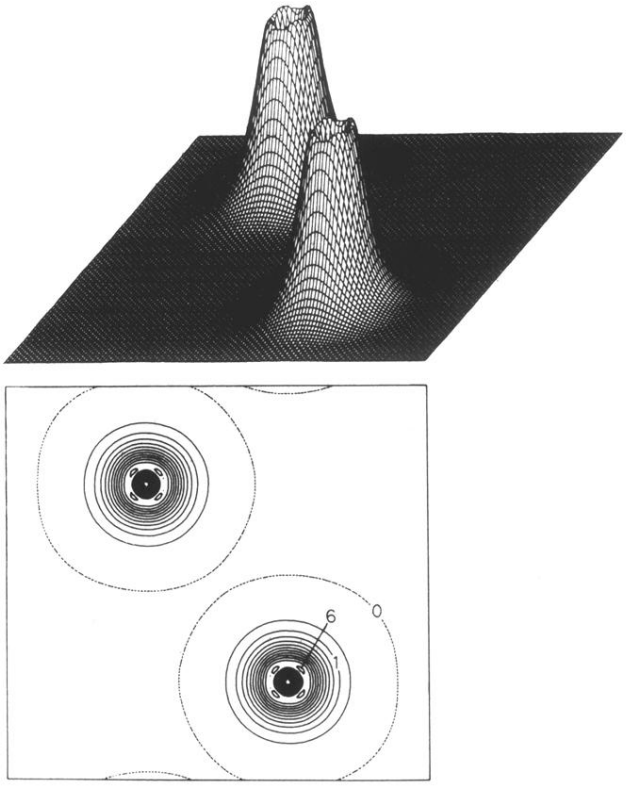

FIG. 12. Spin densities of hcp Co in the $(11\bar{2}0)$ plane. Units of $0.1e/\text{a.u.}^3$ are used in the contour plot.

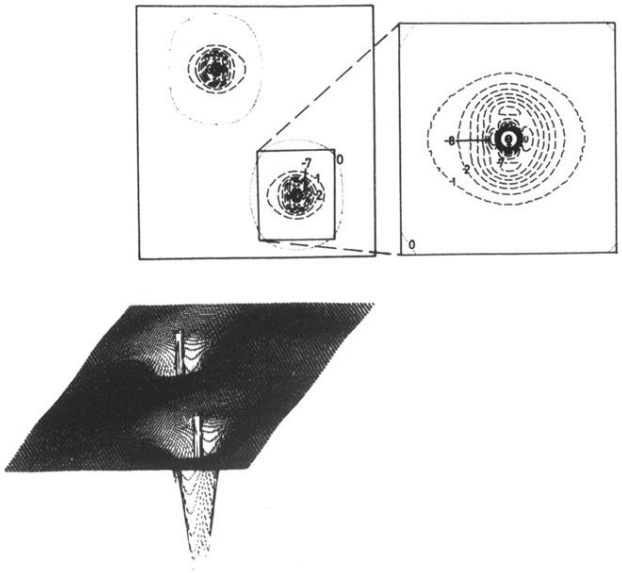

FIG. 4. Difference electron densities of hcp Zn in the $(11\bar{2}0)$ plane. The cutoff of the perspective plot is $0.08e/\text{a.u.}^3$ In the contour plot units of $0.001e/\text{a.u.}^3$ are used.